Available online at www.sciencedirect.com
SCIENCE DIRECT
Cement and Concrete Research 36 (2006) 868 – 878
Cement and Concrete Research

Application of ^{19}F NMR relaxometry to the determination of porosity and pore size distribution in hydrated cements and other porous materials

A.B. Koudriavtsev [a], M.D. Danchev [a], G. Hunter [b,1], W. Linert [c,*]

[a] Analytical Centre, D. Mendeleev University of Chemical Technology of Russia, Miusskaya sq. 9, 125047 Moscow, Russia
[b] University of Dundee, Dundee DD1 4HN, Scotland, United Kingdom
[c] Institute of Applied Synthetic Chemistry, Vienna University of Technology, Getreidemarkt, 9/163AC, A-1060 Vienna, Austria

Received 23 May 2005; accepted 27 September 2005

Abstract

The potential to determine the porosity of cements and other porous materials by employing ^{19}F NMR relaxometry was explored for samples of hydrated Portland cement, white cement and calcium aluminate, filled with Freon 11. The dependence of ^{19}F signal amplitudes on the content of Freon in samples with completely filled pores was linear with a small (<6%) intercept thus allowing a direct determination of total porosity. Additionally it was found that magnetic susceptibility (hence the content of paramagnetic compounds) of the solid can be evaluated from ^{19}F NMR spectra of samples containing exterior liquid. Information concerning pore size distribution can be obtained from the analysis of multiexponential relaxation of ^{19}F nuclei in samples with completely filled pores. Mathematical models employing sets of distributions of relaxation rates have been developed for this purpose. Distributions were assumed to be of a (fixed) square/triangular type allowing for the calculation of moments of any order from the estimated initial value, width of distribution and asymmetry factor. Longitudinal and transverse relaxation were characterised by either single or several continuous distributions of relaxation rates. One of the relaxating phases (assigned to fluid occupying throats connecting the pores) was found to selectively disappear when Freon was evaporated from samples. Another approach is to analyse the dependencies of means and variances of relaxation rates on Freon content. This has been done by employing the two-site relaxation model with a permanent adsorption layer and pore-dependent relaxation enhancement. Simultaneous fitting of dependencies of means and variances of relaxation rates on Freon content yields parameters of pore size distribution and of the dependence of relaxation enhancement on the pore radius. Analysis of experimental data shows agreement between these two approaches.

Keywords: Pore size distribution; NMR

1. Introduction

Porosity is one of the most important parameters of cements and concretes determining as it does the strength of constructions made of these materials. For technological purposes the porosity of these objects is mainly determined from BET adsorption isotherms. In scientific studies, nuclear magnetic resonance methods have been used in the determination of porosity and pore size distribution in cement stones and other porous media employing stepwise freezing of water in pores [1] and multiexponential analysis of NMR relaxation [2]. Chemical shifts of ^{1}H NMR have also been found to be informative with respect to the pore size distribution: signals from organic molecules in small pores of carbonaceous adsorbent were found to be shifted to lower frequencies [3].

Proton ^{1}H NMR measurements on water naturally contained in hydrated cements are connected with some difficulties in the interpretation of experimental data:

The background signal of chemically bound water and of water in the so-called gelphase overlaps with that of the capillary water both in frequency domain and in the relaxation rate scale. It is therefore difficult to evaluate the volume of pores excluding the gel-phase. Stepwise freezing out of water in pores involves redistribution of H_2O molecules among these phases as well as between pores of different size. This redistribution affects the state of gel-phase and hence the original state of cement stone.

* Corresponding author.
E-mail addresses: akoudri@online.ru (A.B. Koudriavtsev), wlinert@mail.zserv.tuwien.ac.at (W. Linert).
[1] We regret to inform that Prof. Hunter passed away in May 2002.

0008-8846/$ - see front matter © 2005 Elsevier Ltd. All rights reserved.
doi:10.1016/j.cemconres.2005.09.015

Recently a novel method of NMR-porosimetry based on Fluorine-19 NMR has been suggested [4]. In this method a specimen of porous material dried to a technologically required water content was filled with an inert fluorine-containing liquid (Freon or any fluorinated hydrocarbon as well as SF_6) and the extrapolated signal amplitude of ^{19}F resonance is measured yielding an estimate of total porosity. The pore size distribution is estimated using the multi-exponential analysis of ^{19}F longitudinal and transverse relaxation. This method has the advantage of having no background signal interfering with the direct determination of signal intensity. The sensitivity of ^{19}F NMR is practically the same as that of ^{1}H NMR, therefore no problems are expected to arise in detecting small amounts of molecules in micro-pores. Moreover, the molecules of fluorinated compounds mentioned above do not chemically interact with the surface of solids and therefore the free induction decay from Freon molecules in micro-pores is longer and easier to detect than that of water.

In this paper a detailed analysis of a study of ^{19}F relaxation in porous systems employing Freon 11 as filling liquid and samples of hydrated Portland cement (pc) white cement (wc) and calcium aluminate (ca) as porous solid is given.

2. Experimental

Fluorine—19 NMR saturation—recovery (80 $\pi/2$ saturating pulses train) curves have been obtained at 188.3 MHz and 296 K using a Bruker CXP-200 spectrometer equipped with a modified high power probehead that provides for the insertion of a 20 mm o.d. sample. The $\pi/2$ pulsewidth of ^{19}F resonance varied within 5–8 μs depending on the sample size and electric properties.

The number of points in the saturation–recovery delay scale was 26 which included four groups of four parallel measurements at $\tau = 4$, 32, 256 and 2000 ms. Parallel measurements yielded the variance of reproducibility of experimental data according to which the adequacy of the fitting of re-equilibration curves was evaluated. Effects of transverse relaxation (arising mainly from the magnetic inhomogeneity of the solid) were taken into account by using calculations from 4 to 8 initial points of each FID. The effective transverse relaxation rate R_2*, i.e. the rate constant of free induction decay was thus measured and not the spin-lattice relaxation rate. However, for simplicity sake we drop the asterisk sign in the formulae below.

The combination of R_1 (SR) R_2 (FID) measurements provided for an increase in resolution power with respect to different phases present in the sample. Additionally phases were characterised by their resonance frequencies (see below) which also increased the resolving power of the employed method. Well-tuned spectrometers of the CXP-type equipped with cryo-magnet provide for a high stability of the NMR signal yielding the required high accuracy of amplitude measurements. The reproducibility error determined from parallel measurements was of the order of 10–15 units at the highest measured amplitude of ca. 10,000 units (each measurement involved at least 4 accumulations at the digital resolution 12 bit).

Hydrated cement samples were prepared from a commercial Portland cement (M-400, Shurov plant) and white cement (Shurov plant). A sample of calcium aluminate was kindly supplied by Prof. T.V. Kouznetsova. Water-to-cement ratio was 0.5 in all cases. Samples (17 mm o.d. and 18–25 mm height) were hydrated for 7 days in a moist atmosphere and stored at ambient conditions.

Before measurements, samples of cement stone were evacuated to the residual pressure 0.1 mm Hg for 1 h in standard 20 mm NMR sample tubes.[2] Freon 11 (Merck) was then adsorbed from the gaseous phase and eventually added, in excess, in liquid form. Sample tubes were fitted with a valve allowing for the release of gaseous Freon. Before each measurement some amount of Freon was allowed to escape and its actual content was determined by weighing. The loss of Freon during a single NMR measurement (with closed valve) was negligibly small (less than 2 mg).

3. Mathematical model of multi-exponential relaxation

In order to correctly estimate the initial amplitude of an FID (proportional to the number of resonating nuclei in a sample) one has to analyse the decay of an NMR signal both in real time (t) and saturation–recovery delay time (τ). Such an analysis implies a knowledge of the longitudinal (R_1) and transverse (R_2*) relaxation rates and their distribution. The problems of the determination of the total porosity and of pore size distribution are therefore closely bound together.

It is generally assumed [5–7] that the distribution of relaxation rates of liquids filling the pores of a solid reflects the distribution of pore radii. This rule is based on the assumption of fast exchange of molecules between bulk liquid and adsorption layer within a pore [5]. The observed non-exponential relaxation reflects therefore the existence of pores of different relaxation efficiency slowly exchanging molecules containing resonating nuclei. If the structure of the adsorption layer is identical in all pores then the relaxation rate in a pore depends exclusively on the surface-to-volume ratio. However, the multi-exponential relaxation of water protons was observed even in controlled pore glasses saturated with water [7]. Such behaviour can be interpreted as indicating a slow exchange between free and bound water within a pore (not very probable) or to inhomogeneous distribution of paramagnetic centres.

In some cases the distribution of relaxation rates can be represented as a continuous spectrum [6], in some instances, however a discrete set of δ-functions is a better approximation [6,7]. It was suggested that slow exchange between free and bound water is better described by a discrete spectrum whereas slow exchange between pores is characterised by a continuous

[2] By evacuating a sample of cement stone for 1 h one removes the gaseous phase but the gel-phase and chemically bound water remains intact because of a very slow rate of water redistribution among the hydrated cement phases (the time of half conversion varies from weeks to months).

distribution [7]. Generally speaking a set of δ-functions can be a good approximation of a system having a limited number of sites with drastically different relaxation rates. If a relaxation rate varies gradually from site-to-site then a continuous distribution of relaxation rates is a better model.

Both these types of variations can be present in a cement stone. We have developed therefore a combined model employing a *set of distributions* of relaxation rates. Each distribution is supposed to be narrow which allows one to use polynomial expansions and *directly estimate central moments* of such a distribution. This accounts for gradual variations of properties. On the other hand employing several distributions provided for an adequate description of sites with drastically different relaxation rates (such as macro- and micro-pores).

For a system exhibiting a distribution of relaxation rates a saturation–recovery curve of a point in an FID can be described as:

$$A(t,\tau) = A_0\cos(\omega t)e^{-\bar{R}_2 t}\sum_i x_i e^{-\Delta R_{2i} t}\left(1-\rho e^{\bar{R}_1\tau}e^{-\Delta R_{1i}\tau}\right) \quad (1)$$

where A_0 is the initial extrapolated amplitude proportional to the number of nuclei in a sample, $\bar{R}_1, \bar{R}_2$ are mean values of relaxation rates, ω is the resonance frequency supposed to be identical for all nuclei in a phase. For a narrow distribution the deviations of R_1 and R_2 from their mean values are small ($\Delta R_{1i}\tau<1$ and $\Delta R_{2i}t<1$) and corresponding exponential in (1) can be expanded into series:

$$A(t,\tau) = A_0\cos(\omega t)e^{-\bar{R}_2 t}\sum_i x_i\left(1-\Delta R_{2i}t+\frac{\Delta R_{2i}^2 t^2}{2!}-\cdots\right) \times\left[1-\rho e^{-\bar{R}_1\tau}\left(1-\Delta R_{1i}\tau+\frac{\Delta R_{1i}^2\tau^2}{2!}-\cdots\right)\right] \quad (2)$$

From ((2)) one straightforwardly obtains[3]:

$$A(t,\tau) = A_0\cos(\omega t)e^{-\bar{R}_2 t}\left[\left(1-\rho e^{-\bar{R}_1 t}\right)\times\left(1+\frac{\overline{\Delta R_2^2}}{2!}t^2-\frac{\overline{\Delta R_2^3}}{3!}t^3\ldots\right) -\rho e^{-\bar{R}_1\tau}\left(\frac{\overline{\Delta R_1^2}}{2!}\tau^2-\frac{\overline{\Delta R_1^3}}{3!}\tau^3+\ldots+\overline{\Delta R_1\Delta R_2}\tau t -\frac{\overline{\Delta R_1^2\Delta R_2}}{2!}\tau^2 t-\frac{\overline{\Delta R_1\Delta R_2^2}}{2!}\tau t^2+\ldots\right)\right] \quad (3)$$

Eq. (3) shows that the re-equilibration of nuclear magnetisation can be viewed as a perturbed mono-exponential process with additional polynomial terms containing central moments of distributions of relaxation rates as coefficients. Mono-exponential parts are actually multiplied by generic functions of the moments of distributions of R_1 and R_2. The terms:

$$\overline{\Delta R_1\Delta R_2}\tau t-\frac{\overline{\Delta R_1^2\Delta R_2}}{2!}\tau^2 t-\frac{\overline{\Delta R_1\Delta R_2^2}}{2!}\tau t+\ldots^2 \quad (4)$$

[3] Bearing in mind that means of the deviations <ΔR> are zero.

reflect correlations between ΔR_{1i} and ΔR_{2i}. These terms are zero for statistically independent ΔR_{1i} and ΔR_{2i}. In general, the rates of longitudinal and transverse relaxation are *not* independent and one can therefore expect some contribution from terms shown in ((4)). In order to be able to neglect correlation coefficients we have used limited numbers of points in FID's so that $\overline{\Delta R_2\Delta R_1}t\tau << 1; \overline{\Delta R_2^2\Delta R_1}t^2\tau << 1$, and so forth. In such a case:

$$A(t,\tau) = A_0\cos(\omega t)e^{-\bar{R}_2 t}\left(1+\frac{\overline{\Delta R_2^2}}{2!}t^2-\frac{\overline{\Delta R_2^3}}{3!}t^3\ldots\right) \times\left[1-\rho e^{-\bar{R}_1\tau}\left(\frac{\overline{\Delta R_1^2}}{2!}\tau^2-\frac{\overline{\Delta R_1^3}}{3!}\tau^3+\ldots\right)\right] \quad (5)$$

Fitting an experimental re-equilibration curve to ((5)) *in principle* yields estimates of the moments of distribution of relaxation rates. This works for the first two terms of expansion yielding means and variances of relaxation rates [8]. However, when higher order terms are to be taken into consideration *the interpretation of the results of fitting becomes ambiguous*. For example, several re-equilibration curves obtained in our experiments can be fitted to ((5)) with $\overline{\Delta R_1^2}=0$ but a non-zero $\overline{\Delta R_1^3}$. These estimates do not have any physical meaning and are therefore merely coefficients of a regression equation.

Such ambiguities have been avoided by regularising the fitting algorithm, viz. by choosing a fixed type of a feasible distribution. An even distribution ('square' distribution function in Fig. 1A) of relaxation rates in the range from R_0 to $R_0+\sigma$ is characterised by the following moments:

$$\bar{R}=R_0+\frac{\sigma}{2};\overline{\Delta R^2}=\frac{1}{12}\sigma^2;\overline{\Delta R^3}=0;\overline{\Delta R^4}=\frac{1}{80}\sigma^4;\ldots \quad (6)$$

Possible asymmetry of the actual distribution has been taken into account by using triangular distributions (Fig. 1B, C) characterised by:

$$\bar{R}=R_0\pm\frac{1}{3}\sigma;\ \overline{\Delta R^2}=\frac{1}{18}\sigma^2;\ \overline{\Delta R^3}=\pm\frac{1}{135}\sigma^3;\ \overline{\Delta R^4}=\pm\frac{1}{135}\sigma^4\ldots \quad (7)$$

Both these types of distribution can be written using one general formula in terms of *two parameters*: the width of distribution σ and asymmetry coefficient s (Fig. 1D):

$$f(R)=\frac{2}{(s+1)\sigma}\left(1+\frac{s-1}{\sigma}R\right) \quad (8)$$

in which the *initial relaxation rate* (third parameter) of the distribution is assumed to be zero ($R_0=0$). All non-central moments of this distribution are completely defined by σ and s:

$$\overline{R^i}=\frac{2\sigma^i}{(i+1)(i+2)}\left(1+\frac{is}{s+1}\right) \quad (9)$$

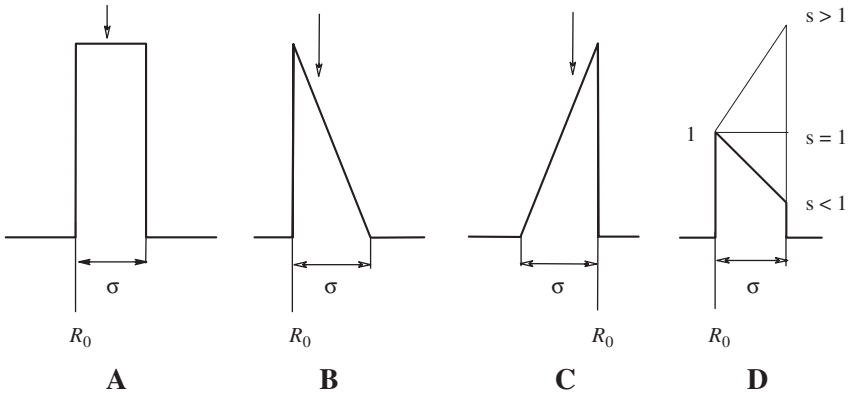

Fig. 1. Square (A) and triangular distributions corresponding to positive (B) and negative (C) third moments. Distribution (D) simulates these types depending on the value of the parameter s. Vertical arrows show positions of the mean relaxation rate.

Central moments are obtained from non-central ones by employing the well-known equation:

$$\overline{\Delta R^n} = \sum_{i=0}^{n} C_i^n \left(-\overline{R^1} \right)^i \overline{R^{n-i}}$$

$$= \sigma^n \sum_{i=0}^{n} C_i^n \left(-\frac{1+a}{3} \right)^i \frac{2[1+(n-i)a]}{(n-i+1)(n-i+2)} \qquad (10)$$

where:

$$a = \frac{s}{s+1}; \quad C_i^n = \frac{n!}{i!(n-i)!} \qquad (11)$$

These moments that arise from the two parameters (σ and s) can be used in the general regression Eq. (5) thus containing any number of expansion terms. In practice it is advisable to use a limited number of terms providing for the independence of estimates on the number of terms. In our calculations it was sufficient to use 10 terms of expansion in ((5)). A square/triangular distribution can be substituted by the gamma-distribution, however the speed of computation in this case is much slower which is not convenient for the regression of large arrays of data. Gamma-distribution can be advantageously used in the cases when the number of computations is not large (see Section 4.3).

The suggested method combines the advantages of the multi-exponential analysis and that of continuous distributions characterised by their moments. The problem of multiple solutions is solved by employing narrow distributions of fixed types. Fitting of experimental data to Eq. (5) involves the optimisation of a not very large number of parameters. Parameters of longitudinal (R_1) and transverse (R_2) relaxation have been estimated from virtually independent sets of experimental data (SR train and FID). In the case of two distributions one has to estimate a double set of 8 parameters: viz. the extrapolated amplitude (A_0), resonance frequency (ω), initial relaxation rates (R_{01}, R_{02}), widths of distribution (σ_1, σ_2), and asymmetry coefficients (s_1, s_2). Values of mean relaxation rates $\left(< R_{1,2} > = R_{01,02} + \overline{R_{1,2}} \right)$ and their variances $\left(V(R_{1,2}) = \overline{\Delta R_{1,2}^2} \right)$ have been computed from these estimates according to Eqs. (9)–(11). In many cases R_2 relaxation was characterised by a single relaxation rate and not a distribution, which decreased the number of adjustable parameters. The regression procedure usually converged very rapidly yielding descriptions with F-criteria of the order 1.1–1.5. When further increase of the number of distributions did

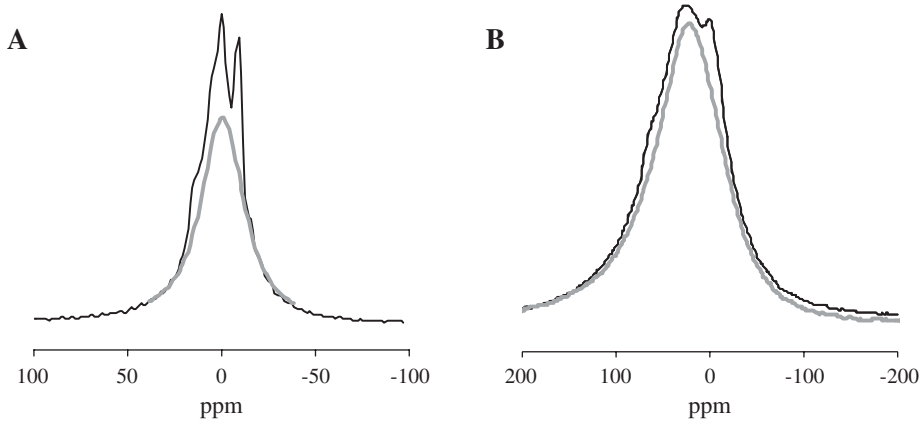

Fig. 2. ^{19}F NMR spectra of Freon in samples of wc (A) and pc. Upper curves are from samples containing an excess (exterior) liquid; lower curves correspond to complete filling of pores.

Table 1
Parameters of investigated samples of hydrated cements

	Maximal amount of Freon, g	Freon content G_F/G_{cem}	A_0, arb.u.	Total porosity, cm^3/g	Invisible Freon, %	$\chi_v\ 10^6$	Fe_2O_3, $\%_w$	$<R_1>$ at complete filling s^{-1}	$V(R)/R^2$ at complete filling
pc	3.120	0.301	15,430	0.201	4.2	282	11.9	2.06	0.06
wc	2.480	0.314	12,408	0.210	11.4	38	1.64	3.80	1.52
ca	1.057	0.131	5005	0.088	25.9	6.51	0.24	0.67	4.27

not improve the regression error (F-criterion) the solution was considered as found.

4. Results and discussion

4.1. Total porosity

Samples containing a visible excess of Freon (exterior liquid) yield specific ^{19}F spectra with additional 'doublet' signals, Fig. 2. This doublet splitting is proportional to the difference of the magnetic susceptibilities of liquid and solid and can be used to estimate the content of paramagnetics in the solid [11,12] (see below).

When Freon was allowed escape, exterior liquid was evaporated and the moment of disappearance of doublet signals corresponds to the complete filling of pores. Total porosity can then be determined from the weight of such a sample as well as from calibrated extrapolated signal amplitude. Results of such determinations for pc, wc and ca are shown in Table 1.

When the extrapolated signal amplitude, A_0, is calibrated using samples of pc, wc and ca completely filled with Freon the calibration chart is a straight line with a small (ca. 6% of the total Freon content) intercept (Fig. 3A). Calibration using samples of cement stones with varying Freon contents yields calibration charts (Fig. 3B) pointing to larger intercepts corresponding the amounts of the 'NMR invisible' Freon varying from 4% (pc) to 25% (ca), of the maximal amount, see Table 1.

The doublet splittings of ^{19}F lines in samples containing exterior liquid yields information on the content of paramagnetics in solid. The distance between 'doublet' peaks is proportional to the volume magnetic susceptibility of the solid sample [11,12]:

$$\Delta \approx \frac{4\pi}{3}\left(\chi_{vsample} - \chi_{vFreon}\right)\frac{r^2_{sample}}{r^2_{tube}} \approx \frac{4\pi}{3}\chi_{vsample} \qquad (12)$$

The percentage of paramagnetics (as Fe_2O_3) calculated from the obtained values of χ_v is shown in Table 1. The variation of the content of Fe_2O_3 qualitatively agrees with the average compositions of commercial cements, however the absolute content of Fe_2O_3 in pc is double the allowed amount of Fe_2O_3 in pc clinkers. This disagreement shows that the demagnetisation factor $4\pi/3$ in ((12)) derived for an infinitely long cylinder is not valid for actual samples. However these data supply correct information on the relative content of paramagnetic compounds in cements.

4.2. Distributions of relaxation rates

To a first approximation the distribution of relaxation rates (hence pore size distribution) can be characterised by averaged means $<R_1>$, and relative variances $V(R_1)/<R_1>^2$ in samples with completely filled pores shown in the last two columns of Table 1. As expected, the mean relaxation rates in samples containing paramagnetic impurities (pc, wc) are higher than in the essentially diamagnetic ca. However the relaxation rate in

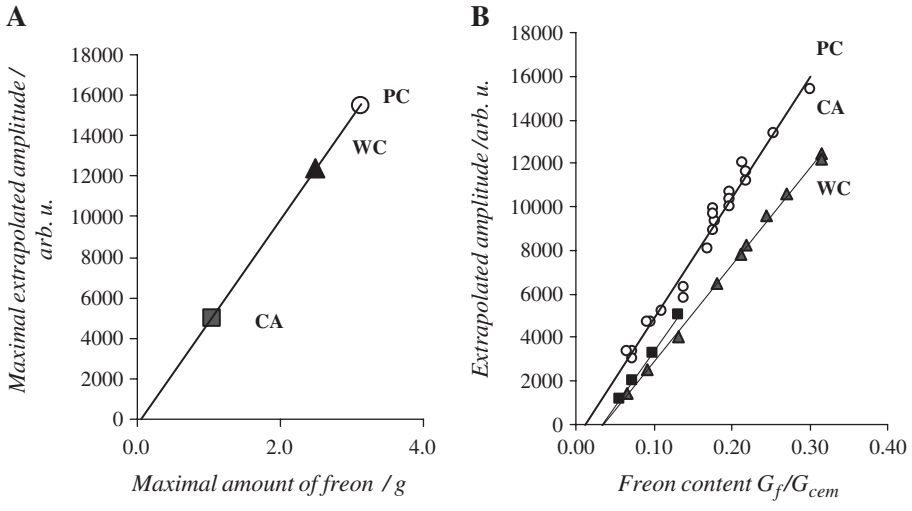

Fig. 3. Dependencies of extrapolated amplitudes of NMR signal on Freon content. Graph (A) corresponds to samples with completely filled pores. Graph (B) shows dependencies on Freon content for each porous medium.

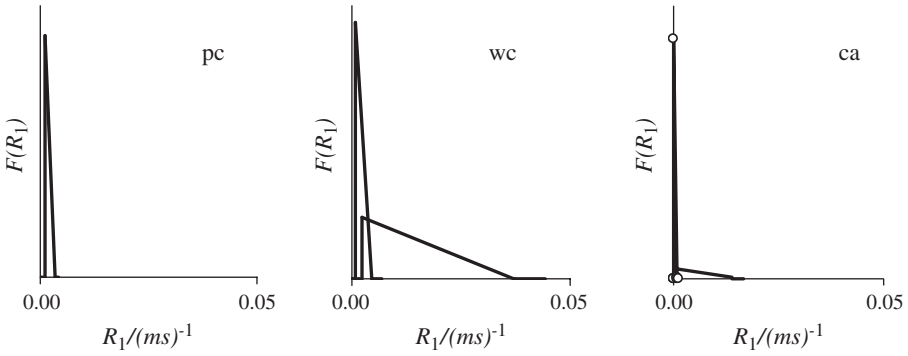

Fig. 4. Shapes of distributions of longitudinal relaxation rates in samples with completely filled pores. Intensities of broader components are multiplied by 10 (wc) and 20 (ca).

pc is considerably smaller than that in wc, containing about 10 times smaller amount of paramagnetic components. This apparently arises from larger diameter of pores in pc compared to those in wc.

Relative variance of relaxation rates in samples with completely filled pores $V(R_1)/<R_1>^2$ characterises the width of distribution of relaxation rates: it increases in the order pc < wc < ca. Similar conclusions will be made from the dependencies of $<R_1>$ and $V(R_1)$ on Freon content (Section 4.3).

Next the shapes of separate distributions of relaxation rates required for the adequate description of experimental re-equilibration curves of samples with completely filled pores can be compared. The decaying triangular distributions ($s<1$, Eq. (8)) describe experimental data better than square ($s=1$) or rising triangular ($s>1$) distributions. In most cases, values of s are close to zero (complete decay of distribution function at the end of the range). Relaxation in samples of pc can be described by one R_1-distribution and one R_2-distribution (one-phase relaxation, Fig. 4, left-hand graph).

In samples of wc and ca a two-phase relaxation is observed each phase being characterised by a distribution of R_1, single R_2 and a single resonance frequency (ω). These phases are mainly distinguished by their frequencies ω and/or transverse relaxation R_2 rates.

Separation into two 'phases' in wc only takes place at large Freon contents (above $G_F/Gcem=0.18$). At lower Freon contents, relaxation becomes one-phase. Fig. 5 shows the dependencies of mean relaxation rates and populations of phases in wc with varying Freon content. The most populated relaxating phase in wc has lower R_1 values. It can therefore be assigned to liquid in macro-pores. This phase disappears in parallel with the decreasing Freon content (see Fig. 5). Population of the second phase, characterised by higher R_1, remains approximately constant over the range of the coexistence of these phases. *The relaxating phase corresponding to liquid in macro pores is thus selectively removed when Freon is allowed to evaporate*.

Relaxation in ca can be separated into two phases over the whole studied region of Freon contents. The slower relaxation phase (95% to 80% of the total Freon) was selectively removed when Freon was allowed escape from sample. The mean R_1 of this phase is close to the longitudinal relaxation rate of bulk liquid Freon (0.51 and 0.37 $(ms)^{-1}$, respectively) in agreement with a very low content of paramagnetic impurities.

The behaviour of R_1- and R_2-distributions in pc at varying Freon content (see Fig. 6) was found to be different: the width of the distribution of R_2 increases with the decreasing Freon content while the width of R_1-distribution decreases (on the

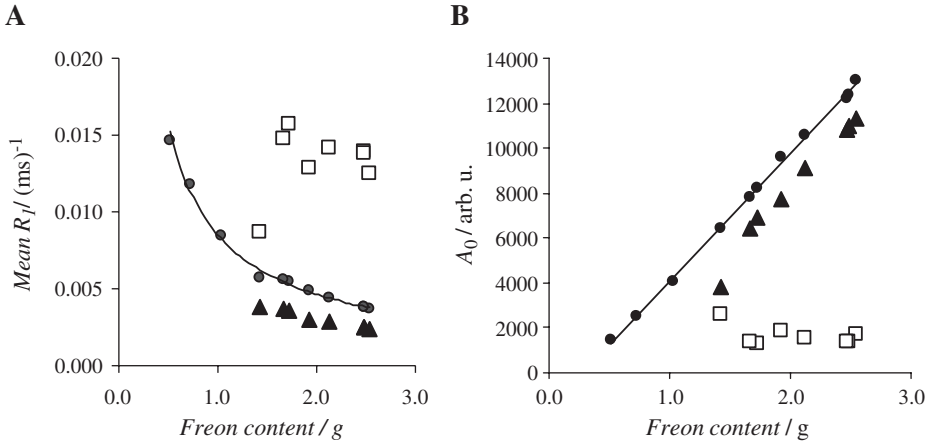

Fig. 5. Mean relaxation rates (A) and extrapolated amplitudes (B) of two relaxating phases (squares and triangles) in wc at different Freon content (grams of Freon per actual sample). Trendlines show the data averaged over all phases.

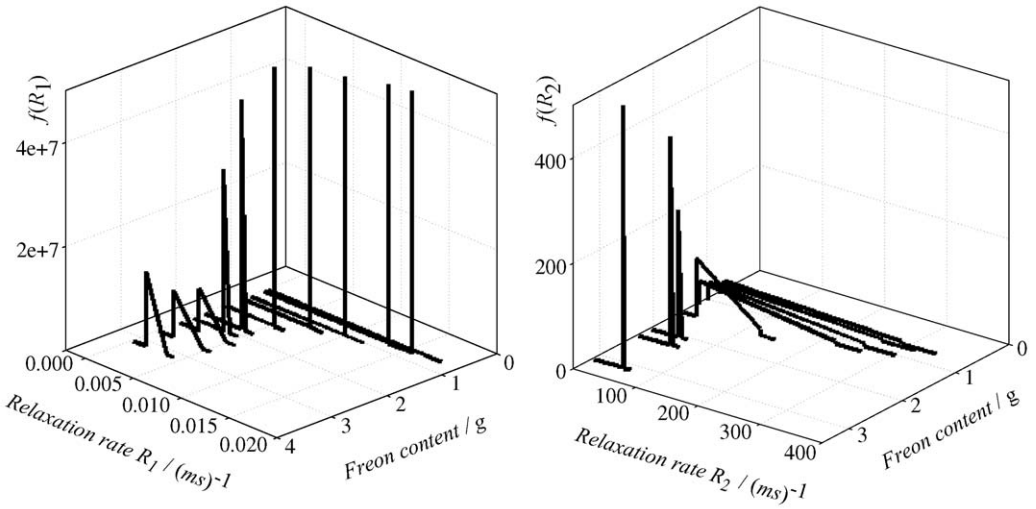

Fig. 6. Distributions of longitudinal and transverse relaxation rates in pc at different Freon content. The first three narrow R_2 distributions (right hand graph) are plotted on a different scale (diminished). The narrow R_1 distributions (left hand graph) are cropped. The Freon content is measured in grams of Freon per actual sample.

absolute scale the narrowest distribution of R_2 is nevertheless wider than the widest distribution of R_1). The origin of such behaviour lies in the actual mechanisms effecting longitudinal and transverse relaxation.

Liquid Freon in spatially distant clusters of pores (Fig. 7) may have considerably different resonance frequencies due to the magnetic field gradient created by a paramagnetic solid. This difference in resonance frequency ($\Delta\omega = \omega_1 - \omega_2$) contributes towards transverse relaxation (R_2) and at slow exchange rate (empty connecting pores, Fig. 7) towards the width of R_2 distribution.

When connecting pores are filled, molecular exchange between clusters is fast and the difference in resonance frequencies, does not contribute towards the width of R_2-distribution. Longitudinal relaxation (R_1) is unaffected by resonance frequencies: it is exclusively determined by the rate of molecular motion and by interaction with paramagnetic centres.

The critical Freon content, below which the width of R_2 distribution sharply increases, can therefore be identified with the situation when connecting macro-pores are nearly empty. In wc and ca the widths of both R_1 and R_2 distributions decrease with decreasing Freon content. The effects of molecular exchange between sites with different ω do not therefore contribute significantly to R_2. This is in agreement with a smaller content of the paramagnetic component in wc and ca compared to pc, and hence a smaller gradient of magnetic field and $\Delta\omega$.

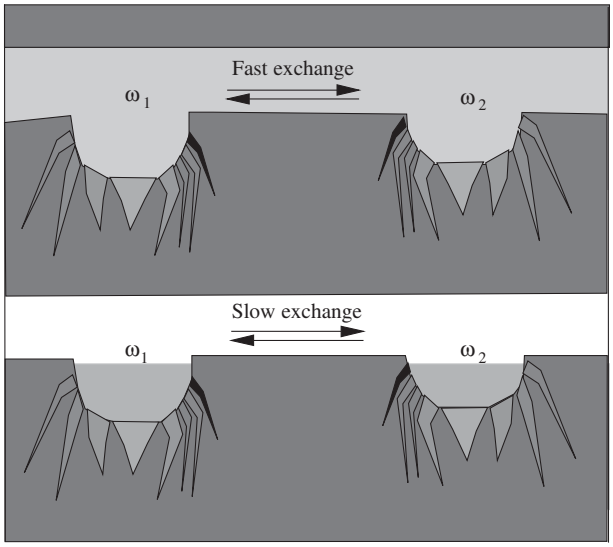

Fig. 7. Filled and partly empty macro-pores. Different shades denote variations in relaxation efficiency.

4.3. Mean relaxation rates and their variances as functions of Freon content

Mean relaxation rates averaged over all phases in a sample can be considered as equal to a virtual rate of mono-exponential relaxation in the same sample but with a very high exchange rate. Experimental $<R_1>$ in our systems are linear functions of inverse Freon content, Fig. 8A, suggesting a very simple two-site relaxation model. According to this model, relaxation occurs at two sites: bulk liquid and 'adsorption layer', i.e. a layer of liquid close to the solid surface in which relaxation is enhanced (compared to that in bulk liquid) by the interaction with paramagnetic surface centres and slower molecular motion. In the framework of this model the average R_1 can be written as:

$$< R_1 > - R_{1b} = \frac{v_{ads}}{V_F}(R_{1a} - R_{1b}) \quad (13)$$

where R_{1a} and R_{1b} are relaxation rates in the adsorption layer and bulk liquid, respectively, v_{ads} is the volume of liquid in the adsorption layer, V_F is the total volume of liquid contained in

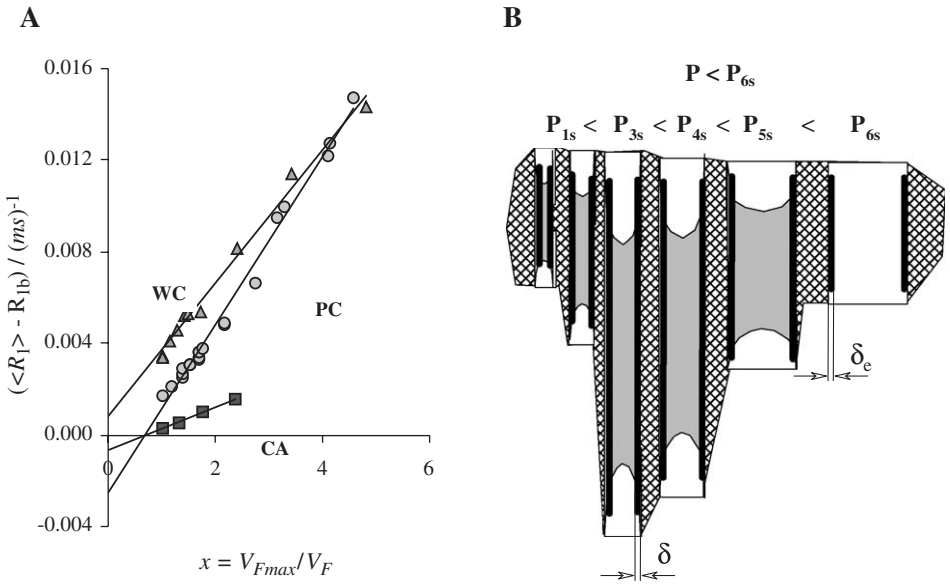

Fig. 8. Experimental dependencies of mean relaxation rates on the inverse Freon content (A). Graph (B) shows schematic picture of the filling of pores thick black lines denoting the adsorption layer.

filled pores and adsorption layer. If the volume of the adsorption layer is constant and R_{1a} is independent of the pore radius Eq. (13) predicts a linear dependence of $<R_1>$ on V_F^{-1} with *zero intercept*. Experimentally however positive and negative intercepts are observed, Fig. 8A.

The condition $v_{ads}=const$ means that the volume of the adsorption layer does not change on the evaporation of Freon from the sample: it must be the same in empty pores and in filled ones. Logically it can be supposed that the adsorption layer in the empty pores is thinner, this leads to positive intercepts such as observed in samples of wc.

Negative intercepts suggest that the actual dependence is curvilinear and one has to consider the mode of filling of the pores by Freon, the effects of pore size distribution and the dependence of relaxation rate in adsorption layer on the pore radius.

The order in which micro- and macro-pores lose the filling fluid depends on whether the latter wets the solid or not. If it does, then the surface of a liquid in a pore is *concave* (Fig. 8B) and the vapour pressure over such a surface is smaller than that over a plane surface. In this case liquid evaporates first from larger pores. The actual vapour pressure is the following function of the radius of curvature of liquid surface in the largest filled pore, r_f [9]:

$$p = p_0 \exp\left(-\frac{2\gamma v_G}{r_f kT}\right) = p_0 \exp\left(-\frac{r_0}{r_f}\right) \tag{14}$$

where p_0 is the vapour pressure over a plane surface, γ is surface tension, v_G is the volume per molecule in the gaseous phase and $r_0=2\gamma v_G/kT$. Our results (see above) show that in wc and ca, Freon is selectively removed from larger pores therefore it *does* wet the solid surface (the case of pc is uncertain).

The theoretical dependence of $<R_1>$ on V_F^{-1} can be defined parametrically, e.g. by defining these variables as functions of the radius of the largest filled pore. For V_F this can be done by integrating from the minimal radius to the radius of the largest filled pore and adding the amount of Freon in the adsorption layer in empty pores:

$$V_F = \int_{r_{min}}^{r_f} V_p(r) r + \int_{r_f}^{r_{max}} V_{ap}(r) r \tag{15}$$

In a similar way the mean relaxation rate must be averaged over $F(r)$, also taking into account, however, the variation of the relaxation enhancement with pore radius:

$$< R_1 > = \frac{\int_{r_{min}}^{r_f} R_{1p}(r) V_p(r) r + \int_{r_f}^{r_{max}} R_{1a}(r) V_{ap}(r) r}{V_F} + R_{1b} \tag{16}$$

in which:

$$V_p(r) = \pi r^2 F(r); \quad V_{ap}(r) = \pi\left[r^2 - (r-\delta)^2\right] F(r);$$
$$R_{1p}(r) = R_b + \frac{V_{ap}(r)}{V_p(r)}[R_{1a}(r) - R_b] \tag{17}$$

In the same manner mean values of R_1^2 can be obtained and the variances of relaxation rates can be calculated as $V(R)=<R^2>-<R>^2$. Quite unexpectedly this model predicts zero intercepts in $<R_1>=f(V_F^{-1})$ irrespective of the shape of $F(r)$ and/or $R_{1a}(r)$. Again positive intercepts are obtained for all possible types of $F(r)$ and $R_{1a}(r)$ if the thickness of the adsorption layer is smaller in empty pores. Negative intercepts are expected for larger adsorption layers in empty pores which does not look probable.

Another explanation of the observed negative intercepts admits the existence at low Freon content of 'NMR invisible'

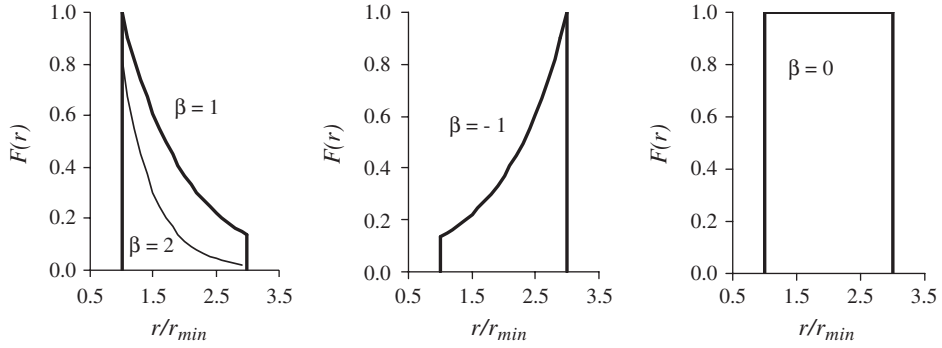

Fig. 9. Gamma-distributions simulated using: $\alpha = 0$, and varying values of β.

species characterised by very fast transverse relaxation. Indeed when all pores are filled the fast exchange between bulk and adsorbed Freon efficiently decreases the transverse relaxation rate and makes all nuclei visible. At low Freon content some parts of adsorbed Freon is separated from bulk liquid and, being characterised by very fast transverse relaxation, becomes 'invisible'.

A linear dependence of mean relaxation rate on V_F^{-1} merely reflects the existence of a permanent adsorption layer in pores and does not yield much information on the pore size distribution. However, the dependencies of the *variance of relaxation rates* are very sensitive towards parameters of pore size distributions and of dependencies of relaxation rate on the pore radius. For such simulations the gamma-distribution [10] is very convenient:

$$F(r) = \left(\frac{r}{r_{\min}}\right)^{\alpha} \exp\left(-\frac{\beta r}{r_{\min}}\right) \tag{18}$$

$$R_{1a}(r) = R_{1a}^{0}\left(\frac{r}{r_{\min}}\right)^{\alpha} \exp\left(-\frac{\beta r}{r_{\min}}\right) + R_{1b} \tag{19}$$

Shapes of this distribution function for several combinations of α and β are shown in Fig. 9. Experimental dependencies of mean relaxation rates $<R_1>$ and relative variances $V(R_1)/<R_1>^2$ can be simultaneously fitted to the

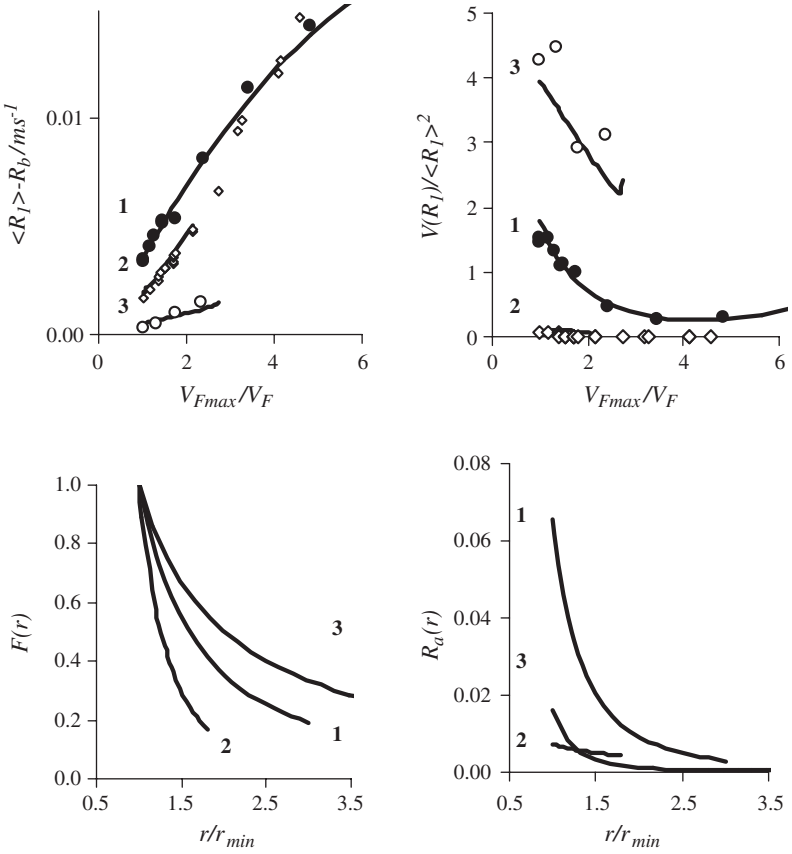

Fig. 10. Simultaneous fitting of mean relaxation rates $<R_1>$ and relative variances $V(R_1)/R_1^2$ as functions of inverse Freon content (V_{Fmax}/V_F) employing the distributions $F(r)$ and $Ra(r)$ shown below. Curves correspond to: 1—wc, 2—pc, 3—ca. Parameters are given in Table 2.

Table 2
Parameters of distributions of pore radii ($F(r)$, $r_{min}=1$) and relaxation rates in adsorbed state ($R_{1a}(r)$) fitted to the experimental data on $<R_1>$ and $V(R_1)$, see Eqs. (18), (19)

	R_{1a}^0/ms^{-1}	σ/r_{min}	δ/r_{min}	$\delta_{empty}/\delta_{filled}$	$F(r)$		$R_{1a}(r)$	
					α	β	α	β
pc	0.007	0.8	0.3	1.3	−3.0	0.0	−1.0	0.0
wc	0.065	2.0	0.2	0.6	−1.5	0.0	−2.9	0.0
ca	0.016	3.3	0.5	1.2	−1.0	0.0	−4.4	0.0

model of an approximately constant adsorption layer as shown in Fig. 10. Parameters obtained for this model are shown in Table 2.

Relaxation rates in paramagnetic-rich pc are unexpectedly lower than in samples of white cement having lower content of paramagnetics. Also the variances of relaxation rates in pc are small.[4] This means that the investigated sample of pc has large, narrowly distributed pores. Low relative variances also require for their explanation large thickness of the adsorption layer (δ) characterised by a very low relaxation rate R_{1a}, smaller even than in samples of diamagnetic ca. This indicates that probably the surface of pores in pc is not wetted by Freon[5] and therefore the interaction of ^{19}F nuclei with paramagnetic centres is hindered.

The width of distribution of pore radii ($\sigma=r_{max}-r_{min}$) *increases* in the order pc–wc–ca. In the same order the thickness of adsorption layer δ (i.e. the range of surface effects on relaxation, see Table 2 *decreases*. The shape of distribution of pore radii in all samples is decaying and is slightly better described by hyperbolic functions ($\beta=0$) than by exponential functions ($\alpha=0$).

The same is true for the dependencies of R_{1a} on pore radius. The fastest decay of R_{1a} is obtained for diamagnetic ca, the slowest for highly paramagnetic pc. This means that in the diamagnetic system only small pores have really high relaxation efficiency whereas in paramagnetically doped wc and pc larger pores also show a high relaxation rate. Relaxation enhancement in ca is thus apparently effected via slower molecular motion, whereas in pc and wc, it originates from interaction with paramagnetic centres.

These data cannot give information on the absolute value of the mean radii of pores, although the relaxation rate in the adsorption layer R_{1a}^0 is dependent on both the mean pore radius and the mechanism of relaxation enhancement in the adsorption layer. The mean pore radius can be estimated from experiments on porous media with known surface concentration of paramagnetic centres and calibrated pores.

[4] Zero variances obtained for smaller Freon contents in pc contradict the model of slow exchange between pores and hence only a part of the experimental curve can be fitted to this model. Data on means and variances in wc and ca can be described over the whole range.

[5] Shapes of dependencies of means and variances of relaxation rates on Freon content in the case of nonwetted surface are similar to those obtained for wetted surfaces.

5. Conclusions

In this paper we have analysed the potential of ^{19}F NMR relaxometry for the determination of the pore size distribution in cement stone. A formalism employing a set of distributions of relaxation rates has been developed and successfully tested. This formalism can be employed in the analysis of multi-exponential relaxation of protons and other nuclei.

Two kinds of tools for the determination of the nature of pore size distribution have been suggested. One involves the analysis of multi-exponential relaxation in samples completely filled with a fluorine-containing liquid. The shape and central moments of distribution can be estimated from experimental data using the developed formalism. The existence of several distributions reflects the presence of several hydrated states whereas parameters of individual distributions can be considered as arising from the pore-size distribution. The use of the moment expansion is a logical consequence of this model and provides for the optimal description of systems with properties gradually changing over a narrow range.

Another approach involves the analysis of the dependencies of means and variances of relaxation rates on Freon content in a sample. Shapes of these dependencies (considered simultaneously) are sensitive towards details of distributions of pore radii and of relaxation rates in the adsorbed state. Using model distribution functions, one can estimate the width of pore size distribution as well as parameters of the dependence of relaxation enhancement on the pore radius.

Total porosity can be determined from the amplitude of ^{19}F NMR signal in samples with completely filled pores. The moment of complete filling can be associated with the disappearance of the characteristic ‘doublet’ signal of exterior liquid. The distance between components of this doublet yields information on the relative amounts of paramagnetics in cement stone.

Acknowledgements

Authors would like to thank Prof. T.V. Kouznetsova (D. Mendeleev University) and Prof. Ryuichi Ikeda (University of Tsukuba) for helpful discussions of the problem. ABK expresses his gratitude to the Royal Society for a grant allowing him a research visit to the University of Dundee. Thanks are further due to the Austrian Science Foundation (Project: 15874-NO3) and to the “Jubiläumsfondes” of the Austrian National Bank (Project 10668) for financial support.

References

[1] S.G. Allen, P.C.L. Stephenson, J.H. Strange, J. Chem. Phys. 108 (1998) 8195;
R. Valckenborg, L. Pel, K. Kopinga, Magnet. Reson. Imaging 19 (2001) 489;
D. Akporiaye, E.W. Hansen, R. Schmidt, M. Stöcker, J. Phys. Chem. 98 (1994) 1926.
[2] J.C. MacTavish, L. Miljkovic, M.M. Pintar, R. Blinc, G. Lahajnar, Cem. Concr. Res. 15 (1985) 367;

L.L. Latour, K.L. Kleinberg, Sezginer, J. Colloid Interface Sci. 150 (1992) 5351;
D.P. Gallegos, D.M. Smith, J. Colloid Interface Sci. 122 (1988) 143;
S. Davies, K.J. Packer, J. Appl. Phys. 67 (1990) 3163.
[3] R.S. Drago, D.C. Ferris, D.S. Burns, J. Am. Chem. Soc. 117 (1995) 6914.
[4] A.B. Koudriavtsev, M.D. Danchev, G. Hunter, W. Linert, Using Fluorine-19 NMR Relaxometry for the determination of pore size distribution in hydrated cements, mortars, concretes and other porous materials, Proc. of the 40th NMR Symposium, 14–16 November 2001, Kyoto, Japan, P70.
[5] E.J. Fordham, A. Sezginer, L.D. Hall, J. Magn. Reson., Ser. A 113 (1995) 139.
[6] K.P. Whittall, A.L. MacKay, J. Magn. Reson. 84 (1989) 134.
[7] K. Overloop, L. Van Gerven, J. Magn. Reson. 100 (1992) 303.
[8] A.B. Kudryavtsev, W. Linert, A.V. Pyatkova, Chem. Phys. 186 (1994) 53.
[9] E.A. Moelwyn-Huges, Physical Chemistry, Pergamon Press, London, 1961.
[10] D.J. Hudson, Lectures on Elementary Statistics and Probability, Geneva, 1964.
[11] C.A. Reilly, H.M. McConnel, R.G. Meisenheimer, Phys. Rev. 98 (1955) 264.
[12] W. Gerger, U. Meyer, V. Gutmann, Monatsh. Chem. 108 (1977) 417.